_____

Histological Evaluation of A unilateral Critical-Sized Mandibular Defect Reconstruction using human dental pulp stem cells by Light Microscope and Real-Time Quantitative PCR

Khalaf, Afaf, Ali[1*], Shamaa, Ali [2] Sabry, Dina, Abd El Fattah [3], Saher S, Mohammed[4]

[1]Oral Biology Department, Faculty of Dentistry, Minia University, Egypt.
[2] Oral Biology Department, Faculty of Dentistry, kafr elsheik University, Minia, Egypt.
[3] Medical Biochemistry and Molecular Biology, Faculty of Medicine, Cairo University, Egypt.
[4] Oral Biology Department, Faculty of Dentistry, Minia University Minia, Egypt.

*Corresponding author's E-mail: afaf_dent_post@med.sohag.edu.eg

Article History	Abstract
	Objective: *To evaluate the osteogenic differentiation potential of human dental pulp stem cells (DPSCs) isolated from the dental pulp of third molar teeth in vitro cultures, and to evaluate the bone regenerative capacity of human dental pulp stem cells (DPSCs) when transplanted into a unilateral critical-sized bone defect in the mandibular bone in vivo after receiving a hydroxyapatite matrix and polylactic-polyglycolic acid (HA/PLGA) scaffold.* ***Material and methods:*** *A total of 18 mandibular defects were made, and three groups (each n = 6) were created. The first group: the transplanted DPSCs implanted in the critical-sized bone defect after receiving (HA/PLGA) scaffold. The second group received only (HA/PLGA) scaffold. The third group, which served as the control, had a critical-sized defect left empty. After characterization, Von Kossa [VK] and Alizarin red staining were employed to identify differentiated osteoblasts at the 14th and 21st days, and histological analyses, as well as polymerase chain reactions (PCR), were also used.* ***Results:*** *It showed that DPSCs had high proliferation potential and typical fibroblastic shape. Additionally, osteogenic differentiation of DPSCs was validated by morphological alterations, histological examination, and the expression of lineage-specific genes confirmed osteogenic differentiation of DPSCs.* ***Conclusion:*** *High proliferation potential and the capacity to differentiate into osteoblasts are two characteristics of DPSCs taken from impacted third molars.*
	Keywords: *Synthetic Scaffold; Tissue Engineering; Dental Pulp Stem Cells; Bone Regeneration*

1. Introduction

Human dental pulp-derived mesenchymal stem cells (HDP-MSCs) are a particularly appealing and feasible way to obtain postnatal mesenchymal stem cells for therapeutic purposes and the field of regenerative healthcare. This is because they naturally possess high proliferative potential and growth rates, the ability to self-renew, and the aptitude for multilineage differentiation [1, 2]. Because of their potential to develop into a wide range of cell types, including osteogenic, adipogenic, odontoblastic, and neural cells. HDPMSCs have a higher proliferative potential and multilineage differentiation capacity, which makes them suitable for both autologous and allograft transplantation in tissue engineering [3].

HDP-MSCs have been used in conjunction with three-dimensional scaffolds to regenerate bone tissue in created critical sized bone lesions. Trials performed in mandibular bone defect's model revealed positive findings of bone formation assessed by immunohistochemistry and histopathology [4]. The

importance of MSCs when transplanted has been shown in in vivo experiments using models of animals, increasing bone formation and consequently the rigidity of the regenerated structures [5].

For the development of the critical size defect model, the choice of animal species is crucial. Rabbits are a better choice because of their quick breeding cycles, handling simplicity, structural and composition resemblance to human mandibles, and high tolerance for mandible faults. Rabbits have an advantage when utilized as a jawbone CSD model because they have adequate alveolar bones in the premolar and/or molar areas to allow for the creation of an appropriate mandibular defect [6].

The implantation of scaffolds or carriers presents one of several potential strategies to facilitate the regeneration of damaged bone tissue [7]. Today, biomaterials utilized to create scaffolds might be either artificial or natural, biodegradable, or not. Natural polymers like chitosan and collagen are used in tissues engineering. Synthetic polymers with varied characteristics, including Poly-lactic acid (PLA), Polycaprolactone (PCL), or Poly (lactic-co-glycolic) acid (PLGA), are used in the engineering of bone tissue [8].

One of the most extensively researched artificial biodegradable polymers, Poly (lactic-co- glycolic acid) (PLGA), is successful owing to its biocompatibility have a series of controllable and appropriate degradation rates compared with tissue growth rate. However, the production of acidic substances during the rapid degradation of PLGA will result in low-local pH and poor toughness. The addition of ceramic materials is beneficial for enhancing cell activity and promoting bone formation [9].

Our work makes use of hydroxyapatite, an osteoconductive substance with porosity comparable to that of natural bone, to encourage the formation of bone tissue across the surface or inside the scaffold's pores [10].

In the present study, we assessed osteogenic differentiation and proliferation capacity of hDP- MSCs in vitro. In addition, it tested its bone regenerative capacity in vivo using osteogenic differentiated DP-MSCs carried on (PLGA/HA) scaffold in a rabbit mandible defect.

2. Materials And Methods
Experimental animals

A total of Eighteen New Zealand white rabbits weighing between 1.5 and 2 kilogrammes were used in the investigation. All animals were treated humanely within the guidance of Minia University's ethical approval committee. Rabbits were obtained and housed in cages at the Faculty of Veterinary Medicine, Sohag University, at a cool room temp away from direct sunlight, guarded from draughts, loud noises, and direct exposure to radiators. The animals were fed commercial pelleted rabbit feed.

Experimental design

A total of 18 mandibular defects were made and three groups were formed: [each n = 6]

☐ **Group 1:** With hydroxyapatite matrix and a polylactic-polyglycolic acid (HA/PLGA) scaffold implanted with human dental pulp stem cells (DPSCs), the critical-sized defect was filled for three months.
☐ **Group 2:** The critical-sized defect filled with HA/PLGA scaffold only for 3 months.
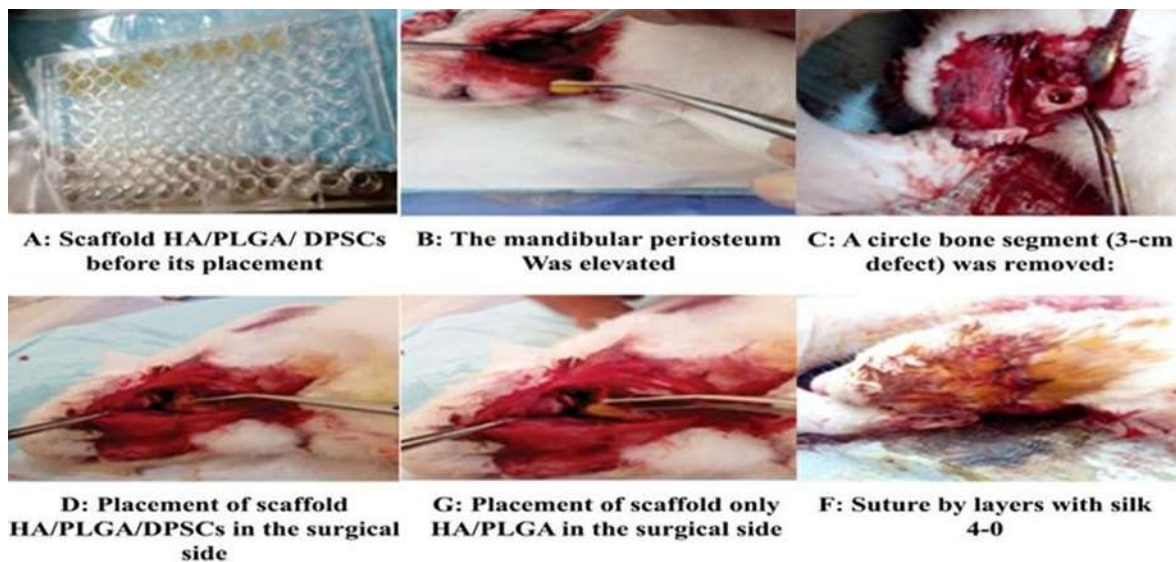☐ **Group 3:** The critical-sized defect left empty and act as a control group For 3 months.

Ethical consideration

Each participant completed a permission form after being apprised of the study's procedures. As part of the ethical council's advice about the conduct of scientific research, all studies were examined and authorized in accordance with the principles for the responsible use of animals in research as a part of the scientific research ethics recommendation of the ethical Minia University **(Approval 22/2/2021: [No. 486]**

In vivo study

Induction of the rabbit's mandibular defect

Each rabbit was starved for 12 hours before surgery. General anesthesia was established and maintained throughout the surgical operation by injecting xylazine (5 mg/kg body weight) and ketamine hydrochloride (35 mg/kg body weight) intramuscularly, [11] .External incision was made in mandibular base of ~2cm by lancet as long as layer dissection, and sub periosteal flap was extended to the muscle layers till reaching the bone . Hard drill #702 with low-speed hand piece was used to generate a circular critical-size defect that was approximately ten millimeters in diameter and three millimeters in height. Constant irrigation with sterile saline solution 0.9 percent was done on all animal models. Using a precise excavator, the bone tissue was eliminated. The flaps were then layer-sutured and properly adjusted. **(Fig. 1)** Postoperative pain was managed by injection of 50 mg buprenorphine/kg each 2 h for the first day [12].

A: Scaffold HA/PLGA/ DPSCs before its placement

B: The mandibular periosteum Was elevated

C: A circle bone segment (3-cm defect) was removed:

D: Placement of scaffold HA/PLGA/DPSCs in the surgical side

G: Placement of scaffold only HA/PLGA in the surgical side

F: Suture by layers with silk 4-0

In vitro study

DPSCs Isolation: The following processes are included in the techniques that are primarily utilized by researchers to find, isolate, multiply, and distinguish DPSCs:

Equipment's:

1. Teeth of healthy people were harvested from teeth of healthy adults.

2. Each patient had their systemic and oral health examined before extraction. Only healthy participants were chosen.

3. Each participant, who was typically a patient that must undergo a third molar extraction, follows a pretreatment with professional dental hygiene action.

4. To decrease microbial flora, the dental crown was coated with 0.3% chlorexidin gel for two minutes before extraction. The cemento-enamel connection was incised with a cylindrical turbine bur using a tiny excavator and cow horn forceps, the pulp was delicately extracted under sterile circumstances, placed in culture medium containers, and transported to the lab in less than two hours.

5. After being extracted, the pulp was immersed in a digestive mixture comprising gentamicin, 3 mg per milliliter, type I collagenase, and four milligrammes per millilitre dispase for one hour at 37 degrees Celsius.

6. Following that, the mixture was filtered through a 40-m filter in a bath of shaking water.

DPSCS Culture:

1. Cells were filtered before being placed in 75-cm3 flasks with filtered valves and cultured in a culture mixture supplemented with 10% fetal bovine serum, 2 mM L-glutamine, 100 U/mL penicillin, and 100 g/mL streptomycin.

2. The medium was replaced twice a week, and the flasks were kept at 37°C with 5% CO2. Just before confluence, cells can be divided into new flasks.

3. The number of passages reached 3rd passage.

4. Stem cells reached at least 3,000,000 per flask. This number was achieved around day 21, when they were still undifferentiated.

Dental pulp stem cell (DPSCs) will be characterized by flow cytometry at the third passage through the evaluation of the expression of the markers that define its phenotype as CD73, CD105, CD90, CD34, and CD45

DPSCs' osteogenic differentiation

In 6-well tissue culture plates with entire expansion culture media, two passages of DPSCs at a concentration of 5×10^4 cells were plated for in vitro osteogenic differentiation. Osteogenic induction media (Osteo life LM-0023, LOT number 05007) mixed with a one percent penicillin- streptomycin solution (Catapricorn PS-B, CP13-1019) was used in lieu of the main culture medium when DPSCs cells reached 80%–90% confluence. Every 3-5 days, the osteogenic differentiation medium was changed out for new media, experiments were terminated after 21 days [13].

By using the Von Kossa stain, osteogenic differentiation is evaluated.

By using "Von Kossa" staining, the differentiation of DPSCs into osteoblasts was evaluated. Briefly, the osteogenic differentiation media was removed after 14 and 21 days of induction, and cells were fixed with 10 percent formalin for fifteen minutes. To stain the cells, a commonly

available Von Kossa staining kit (MASTER TEC STAIN KITS lot No. AAEWD005) was employed. Bright field microscopy was used to view stained cultures and take pictures [14].

Alizarin red staining

The osteogenic induced cultures were stained with alizarin red staining (Cat no 22889). 2% Alizarin Red S was used to stain differentiated DPSCs for 15–30 minutes after they had been fixed with 10% formalin for 15 minutes. Following a thorough deionized water wash, cultures were examined under a light microscope [15] .

Preparation of HA/PLGA scaffolds

50/50 solutions of HA and PLGA were blended in 0.2% chloroform at 25 °C for 24 hours in a 3:1 weight-to-weight ratio. After mixing and dissolving, it was discovered that the HA/PLGA solution was placed over a cylindrical replica mold for two hours at -20 °C before being lyophilized. Small cylinders made of HA/PLGA scaffolds (about 9 mm in diameter and 2 mm in height) were cut to fit the 24 wells' area. DPSCs (5 105, between passages 3 and 6) were introduced into the HA/PLGA scaffold and maintained in DMEM culture conditions at 37 degrees Celsius before being placed in the critical-sized bone fracture of the animal model. [16]. Before placing DPSCs into the animal model's critical-sized bone lesion, they can be kept at 4°C for 24 hours without significantly losing their vitality.

Polymerase chain reaction (PCR)

Polymerase chain reaction was used to assess the expression of genes that are distinctive to a certain lineage. In a nutshell, TRIZOL (Invitrogen) was used to extract RNA after days 14 and 21 of osteogenic induction, and reverse transcriptase (Wizscript cDNA synthesis kit) was used to create cDNA [17]. For PCR, WizPureTM PCR 2X Master Mix was used. The primer pair sequences, and product lengths (bp) are shown in Table 1.

Table [1]: List of used primers and their sequences: -

Gene symbol	Primer sequence from 5′- 3′

RUNX2	F: ATGCATTTAAGATATGGTTGCC
	R: TGGAGTTGGGAAACACTTGA
ON	F: CGAGCTGGATGAGAACAACA
	R: AAGTGGCAGGAAGAGTCGAA
COL I	F: GATGCGTTCCAGTTCGAGTA
	R: GGTCTTCCGGTGGTCTTGTA
GAPDH	F: ATCGTGCGGGACATCAA R: AGGAAGGAGGGCTGGAA

The following PCR conditions were used; denaturation for 5 minutes at 95°C; followed by annealing for 30 seconds at 55°C and extension at 72°C. PCR products were visualized by agarose gel electrophoresis.

Animal euthanasia and sample collection

Euthanasia was performed by anesthetic overdose (ketamine and xylazine) at the 3 months postoperative day. The critical-size bone fracture region was then excised and given to processing slides for further investigation.

Sample examination using microcomputer tomography:

Following sacrifice, the excised bone samples were transferred with a damp cloth to the center of [the Ora-scan. Sohag] for m-CT analysis. Micro-computer tomography (m-CT) equipment (Fan beam Micro-CT) was used to evaluate the samples. The m-CT system's microfocus X-ray source has a maximum voltage of 36 kV and a spot size of 7 mm. The samples were put in a sample container with water in it. They were positioned so that the sample holder's axis and the block's long axis were parallel to each other. With a slice thickness of 120 mm, feed of 60 mm, and pixel size of 60 mm, a high-resolution protocol was used. Depending on the length of the specimens, up to 180 slices were scanned perpendicular to the block. To accurately differentiate between the two tissue types, the ranges and averages of the grey levels distinguishing the scaffold and freshly generated bone were computed. To validate the distinguishing criteria, -CT slices were compared to the corresponding histology slides [18].

Analysis

Histopathological analysis

Following the micro-CT measurements, tissue samples were prepared for histological investigation. The samples were decalcified in Plank-Rychlo's solution for 5 days (MUTO Pure Chemicals Co., Tokyo, Japan), then dehydrated in graded ethanol baths and embedded in paraffin. The implanted samples were cut into 4-m-thick slices using a microtome and stained with hematoxylin-eosin (HE; Sigma, St. Louis, MO) according to specified protocols [19]. To photograph stained slides, a standard light microscope (Leica DM500, Leica Microsystems, Wetzlar, Germany) equipped with a SPOT digital camera (Diagnostic Instruments, Inc., Sterling Heights, MI, USA) was utilized. During the histomorphometric investigation, four spots were chosen at random for each slide, and the new bone formation area of each site was calculated using the Image-Pro plus 6.0 program. (Media Cybernetics, Silver Spring, MI, USA).

Immunohistochemistry analysis:

Histological specimens (4 millimeters thick) were gathered on salinized slides and subsequently kept in an oven at 37 degrees Celsius for a day in order to increase adhesion of the tissue sections under research. After deparaffinization and hydration, sections of histology were marked with a hydrophobic pen and rinsed repeatedly in a buffer solution containing Tween for three minutes. The sections were then immersed in hydrogen peroxide for 10 minutes, phosphate buffer solution (PBS) twice in 3 minutes, and a chemical that inhibited endogenous peroxidase for 30 minutes.

The samples were incubated for a two-hour period with an anti-Col-I polyclonal primary antibody from Santa Cruz Biotechnology in Dallas, Texas, before being washed twice with PBS. They were then incubated for a thirty-minute period with a secondary antibody (anti-rabbit IgG) from Vector Laboratories in Burlingame, California, USA. After this, the samples were washed three times in PBS before being subjected for forty-five minutes to an avidin-biotin complex linked with peroxidase from Vector Laboratories in Burlingame, California, USA. To visualize the bound complexes, a 0.05% 3'3 diaminobenzidine solution was employed, with contrast given by Harris hematoxylin (Vector Laboratories, Burlingame, CA, United States) [20]. The immunomarking for collagen-I (Col-I) was evaluated subjectively and semi-quantitatively. The semi-quantitative study was carried out using a light microscope (Leica Microsystems, Wetzlar, Germany) following the qualitative analysis confirmed the presence of a brownish immunostaining. In a blind study, all analyses were performed by a qualified pathologist. [20] .

Data analysis

The aforementioned information is shown as means and standard deviations. The SPSS 15.0 program was used to analyze the data (SPSS Inc., Chicago, IL, USA). P values under 0.05 were deemed significant, while P values between $P<0.01$ and $P<0.00$ were deemed highly significant.

3. Results and Discussion
In vivo study

Fig 2 [A-B] Macroscopic and radiographic images of the implantation sites at 3 months:

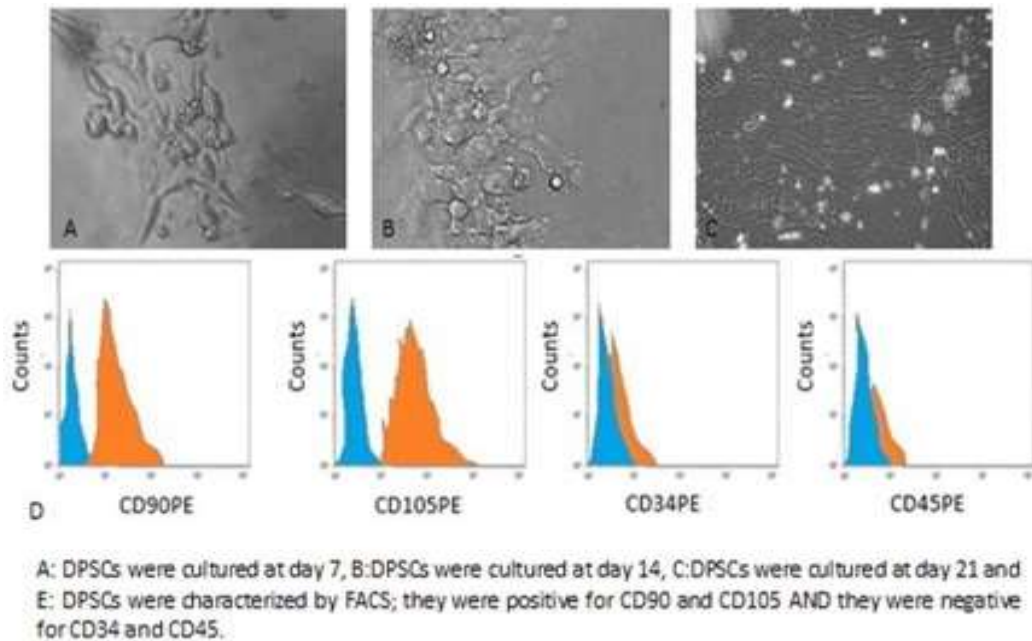A] PLGA/HA/HDPSCs   B: PLGA/HA   c:- control

B]

Figure 2: A: The group I demonstrated the good macroscopic bone repair after three months by filling the defect region with tissue of a firm consistency. (B) Three months after implantation, a significant amount of the leftover scaffold was seen at the defect site in group II, where the defect was partially filled by callus bone. (C) Three months after implantation, the fibrous tissues and failure of ossification in the control defects gave them a mushy consistency.

B: The group I was difficult to distinguish from the original surrounding bone and had a stronger radiopaque signal at the lesion location, indicating higher density of newly formed bone. (B) The defect in group II had a higher radiolucent defect filling, which suggested a less capable matrix creation for the newly created bone. A radiolucent circle was visible inside the control flaws, verifying (C). The lesion is shown as a critical bone defect.

**Human dental pulp-derived mesenchymal stem cells were isolated and characterized (DPSCs): -**

Cells began to proliferate and adhere to the plastic surface of the culture medium after 4 to 7 days. According to **fig. 3,** adherent cells established a monolayer after three weeks and reached 70% - 80% confluence after roughly two weeks of growth. The fibroblastic form and plastic adhering properties of MSCs set them apart. DPSCs were identified by fluorescence-activated cell sorting

[FACS] in flow cytometry; these cells were positive for CD90 and CD105 but negative for CD34 and CD45.

A: DPSCs were cultured at day 7, B:DPSCs were cultured at day 14, C:DPSCs were cultured at day 21 and E: DPSCs were characterized by FACS; they were positive for CD90 and CD105 AND they were negative for CD34 and CD45.

Osteogenic differentiation potential of dental pulp derived mesenchymal stem cells DPSCs

After 14 and 21 days of induction in osteogenic induction media, freshly differentiated osteoblasts developed in numerous layers and stained positively for "Von Kossa" and "Alizarin red S," demonstrating that DPSCs were differentiated into osteoblasts. Alizarin red staining assay was performed for detection of the calcium deposits (mineral deposits) chelate with alizarin forming an alizarin red calcium complex detected as orange-red staining spots as shown in **fig 4.**
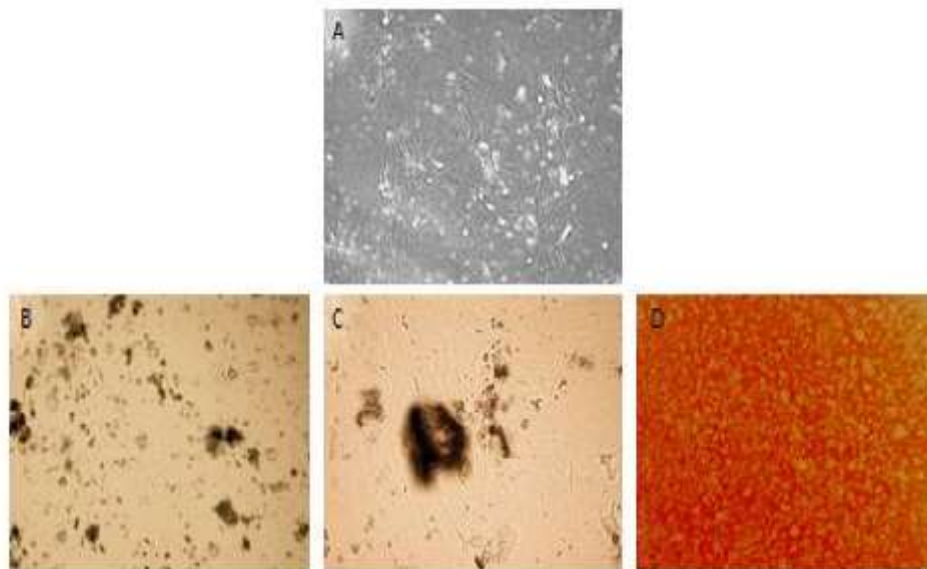
Differentiation potential of DPSCs. A) controlled, B, C) Von kossa staining at day 14 and 21 respectivly, confirming mineral depostion by newly formed osteoblasts D) alizarin red staining at day 21.

Real-Time Reverse Transcription Polymerase Chain Reaction (RT-PCR) is used to assess mRNA expression:

RUNX2, ON, and COL1 mRNA expression levels in differentiated DPSC groups were used to gauge their in vitro osteogenesis. As quantitative benchmarks, the expression levels of several genes in collections of differentiated DPSCs were employed. The osteoblast-specific transcription factor RUNX2 showed strong expression at days 15 and 30 after cell seeding on PLGA/HA scaffolds, which was significantly greater than in other treated and control groups [value was around 3.728516 ($p < 0.05$)]. Osteonectin [ON], another mineralization marker, was consistently expressed in all experimentally treated groups. In addition, the PLGA/HA/DPSCs group displayed a greater expression level (about 3.372864) than the other groups. Lastly, the differentiated DPSCs groups consistently had higher collagen1 expression than the other groups. [Approximately 3.56174 ($p < 0.05$)].

Histological analysis of bone regeneration

The PLGA, HA, and +DPSC specimens showed nearly complete osseous closure of the lesion, with the newly formed bone exhibiting typical organized and mature bone morphology with Haversian systems and identifiable marrow spaces like natural bone. Histological evidence is added to these radiographic findings. Moreover, osteocytes are seen in the newly formed, thickened bone. In addition, considerable numbers of osteoplastic cells can be seen on the surface of the newly formed bone. The PLGA/HA scaffold-only group had a considerable quantity of blood clot in the middle section of the defect as well as the presence of tiny foci of connective tissue with enhanced production of juvenile trabecular bone along the defect borders. Furthermore, the bone deficiency in the control group is mostly filled with connective tissue. In other words, no bone structure is visible after 3 months, and only fibrous scar tissue formation is seen as illustrated in **Fig. 4. [A-B-C].**

Immunohistochemistry was performed to determine Collagen type I expression levels. Immunohistochemistry exhibited strong expression in areas of new bone formation within the defect region from samples treated with the PLGA/HA/HDPS whereas PLGA/HA staining were visible but much weaker. Moreover, no obvious positive staining was observed in the control group as shown in **fig 4 [D-E-F].**

Photomicrographs of decalcified section in the critical sized of mandibular defect in the three experimental groups after 3 months of implantation. (D) PLGA/HA/HDPSCs group showed intense immunoreactivity in areas of new bone formation within the defect region in the osteoid.

(E) PLGA/HA scaffold only group showed the newly formed bone in the central areas of the defect, the osteoblasts along the surface [o.B], and osteocytes[o.c] displayed moderately positive immunoreactivity .Moreover, the connective tissue fibroblasts showed variable staining, [C.T].

(F) The control group showed negative immunoreactivity, and fibrous connective tissue in the bone defect area showed a few positive immunostainings [C.T.]. [Immunohistochemistry of Collagen Type I].
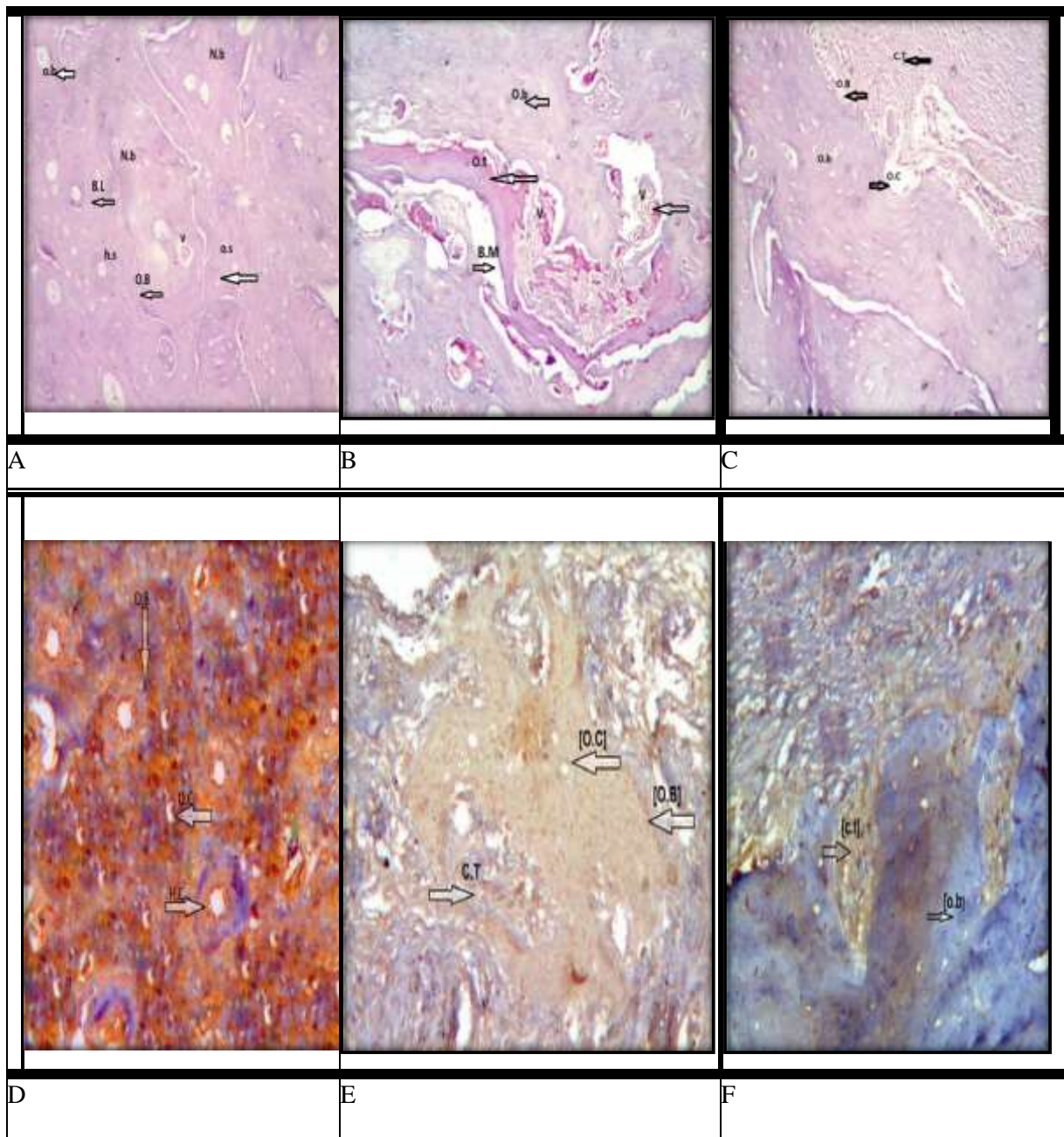
Figure (5): Photomicrographs of decalcified section in the critical sized of mandibular defect in the three groups after 3 months of implantation. (A) PLGA/HA/HDPSCs group showing newly formed compact bone composed of osteon, Haversian canal [H.S] lamellar bone [b.l], osteocyte [O.c] and osteoblast lining the surface of newly formed bone [o.B]. (B) PLGA/HA scaffold only

group showing newly formed osteoid tissue in the central region of the defect with wide bone marrow spaces [B.M] and new vascularization [v] (C) Control group [empty bone defect showing old bone and osteoclast on the surface of the resorbing bone [o.c] and The defect region was filled by osteoblasts on the surface of newly created bone and fibrous tissue scar [F.t]. Hematoxylin and eosin (HE) staining, bar = 40 m, objective increase x10.

Photomicrographs of decalcified section in the critical sized of mandibular defect in the three experimental groups after 3 months of implantation. (D) PLGA/HA/HDPSCs group showed intense immunoreactivity in areas of new bone formation within the defect region in the osteoid.

(E) PLGA/HA scaffold only group showed the newly formed bone in the central areas of the defect, the osteoblasts along the surface [o.B], and osteocytes[o.c] displayed moderately positive immunoreactivity   .Moreover, the connective tissue fibroblasts showed variable staining, [C.T].

(F) The control group showed negative immunoreactivity, and fibrous connective tissue in the bone defect area showed a few positive immunostainings [C.T.]. [Immunohistochemistry of Collagen Type I].

Morphometric assessment:

Area Percentage of new bone formation and bone marrow in the critical sized of mandibular defects in the four experimental groups:

For each group in each test, the mean and standard deviation values were computed. Using the Shapiro-Wilk and Kolmogorov-Smirnov tests to determine if the data were normal, the data revealed a parametric (normal) distribution. One-way ANOVA and the Tukey post-hoc test was used to compare more than two groups in samples from unrelated populations. The cutoff for significance was chosen at P 0.05. With IBM® SPSS® Statistics Version 20 for Windows, a statistical analysis was carried out.
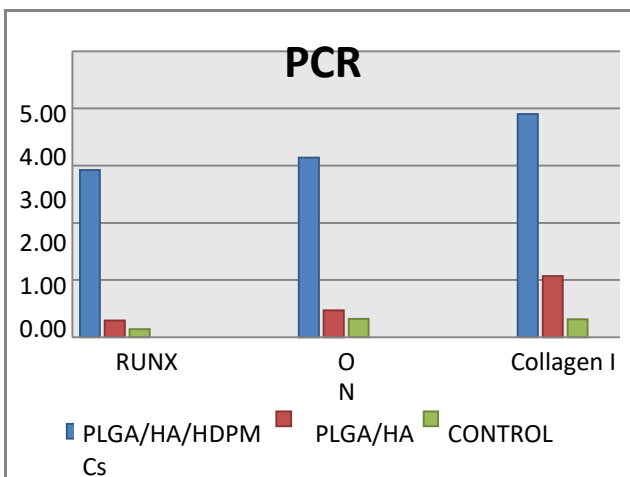

Figure [6] :- A bar chart representing PCR results for different groups in the mean and standard deviation (SD) values of RUNX2 -ON- Collagen
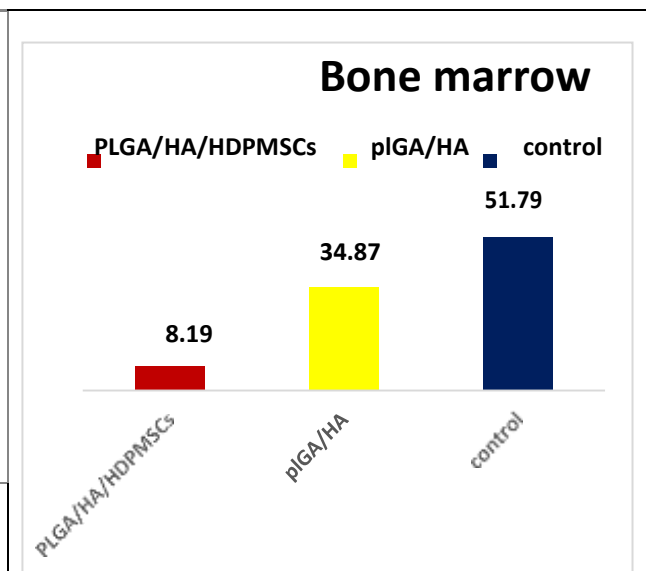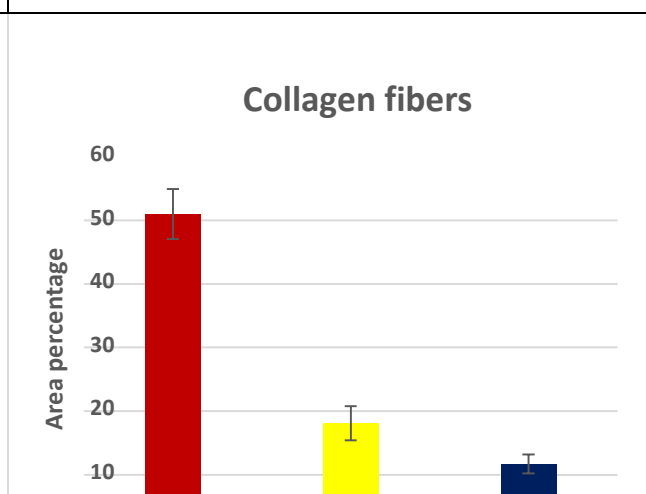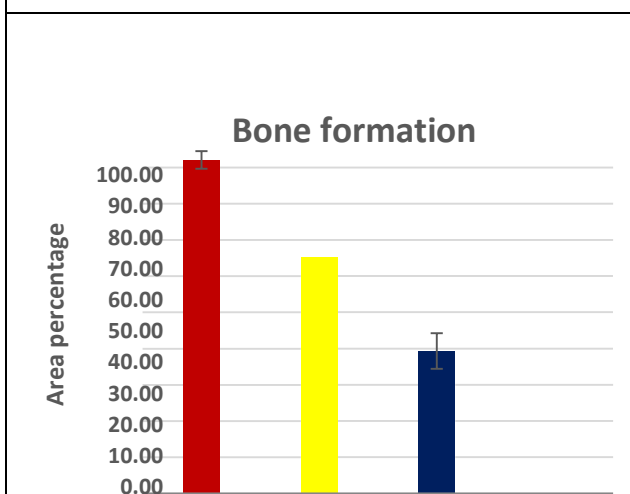

Figure (7): Bar chart representing bone marrow in the three experimental groups

Figure (8) Bar chart representing bone formation for the three experimental groups

Figur (9): Bar chart representing collagen fibers in the three experimental groups

From newly generated bone tissue, total RNA was extracted, and Runx2 primers were used in RT-qPCR, osteonectin [ON], collagen type 1, and GAPDH to represent the differences in the critical size of mandibular defects among the experimental groups of rabbits. The findings demonstrated that there was a statistically significant difference in the mean values between each group. ($p<0.0001$). There was an increasing trend in the experimental groups PLGA/HA/HDPMSCs ($p < 0.05$) While showed a decreasing trend in the scaffold only groups and the empty control groups.

Histological results show that the groups receiving treatment displayed a more developed healing process and showed more new bone formation when compared with the control groups were verified by the histomorphometric analysis. PLGA/HA/HDPMSCs from group [I] displayed 92.09%, PLGA/HA from group [II] 65.16%, and control group 39.28%, respectively. Between (Group 1) and each of (Group II) and (Group III), a statistically significant difference was found where ($p<0.001$) and ($p<0.001$).

Between (Group 1) and each of (Group II) and (Group III), the amount of bone marrow indicated a statistically significant difference, with ($p<0.001$) and ($p<0.001$).

Immunohistochemistry Collagen I result

Immunohistochemistry Collagen I represent the semi-quantitative analysis of the Col-I performed through score. The findings demonstrated significant statistical differences in the amount of collagen fibers present in each examined experimental group. During the three-month trial, the control group had the fewest collagen fibers compared to the PLGA/HA/HDPMSCs and PLGA/HA groups (p 0.001).

The function of bone tissue engineering in regenerative medicine has been the focus of intense research over the last two decades. Technological advancements have enhanced bone repair surgery procedures and orthopedic implants [21]. However, advancements in surgical procedures for bone reconstruction have been hampered by a lack of autologous materials and donor site morbidity [22].

The use of osteoprogenitor cells and scaffolds that can be inserted in vivo at the location of the fractured bone has been recognized as a fascinating prospect for the repair of critical-sized bone defects, with MSCs currently considered to be the most suitable candidates for bone tissue engineering uses [23]. **Dang et al.,** on the opposite hand, found that using stem cells on scaffolds significantly improved and accelerated bone healing [24].

A combination of mesenchymal stem cells and biosynthetic matrix (MSCs) was used. In the present study, homogenous hDPSCs with defined characteristics of MSCs were transplanted with an HA/PLGA scaffold in the surgical field. We studied the effect of HA, PLGA, and HDPSCs on bone regeneration and observed promising results in the accelerated bone regeneration of large defects in the critical size of mandibular defects in rabbits in about 3 months.

Available online at: https://jazindia.com

Because of its desired mechanical characteristics, biodegradability, and biocompatibility, PLGA is an FDA-approved synthetic polymer that has been widely employed for in vitro and in vivo bone regeneration investigations [25, 26]. Even though pure PLGA is biocompatible, its clinical usage for bone regeneration is limited by weak osteoconductivity and inadequate mechanical characteristics. As a result, PLGA is frequently combined with ceramics [HA] to make it more biomimetic and capable of enhancing the growth of bones for tissues engineering and regenerative medical applications [27].

Following primary culture, a subpopulation of cells (DPSCs) with spindle form, fibroblastic shape, and plastic adherent growth were found. MSC characterization standards are established by the International Society for Cellular Therapy (ISCT). These criteria revealed that the cells in our research exhibited CD90 and CD105 while being negative for CD34 and CD45. Previous research [28, 29] found that the CD34 marker was expressed in primitive pluripotent stem cells of both stromal and hemopoietic origin, and it is widely considered as a hemopoietic marker for stem cell populations. in addition, our findings are consistent with those of **Suchánek et al.,** [30] and **Kellner et al.,** [31].

The main culture medium was changed with osteogenic induction media when the DPSC cells achieved 80%-90% confluence for 21 days to evaluate their growth characteristics and osteogenic differentiation ability. They showed excellent differentiation into osteoblasts. In this work, we found considerable morphological changes in induced cultures from fibroblastic to plump and cuboidal-shaped cells. In addition, newly formed osteoblasts formed structured ECM with calcium-rich deposits in vitro, as evidenced by positive staining with "Von Kossa" and Alizarin Red. The findings agreed with those of **Graziano et al.,** [32] and **Kermani et al.,** [33].

On days 14 and 21, PCR was utilized to assess the expression of certain bone-forming gene markers to investigate DPSC differentiation at the mRNA level. Over a 21-day timeframe, the transcription factors RUNX2, osteonectin (ON), and collagen 1 were upregulated in the monolayer of DPSCs under osteogenic conditions. RUNX2 was discovered as an early osteogenesis marker on day 14 and was judged a crucial signal during osteoblast differentiation from DPSCs. RUNX2 also stimulates the expression of ON, an osteogenic differentiation marker. Previous studies assumed that ON is only produced by mature osteoblasts near the conclusion of osteogenic matrix maturation; nevertheless, it may be detected as early as day 14 of osteogenic differentiation.

COL-1 constitutes 90% of the organic matrix. The many osteolytic changes that occur during bone remodeling and collagen breakdown contributed to the identification of COL-1 as a viable bone turnover biomarker. The results we obtained in this experiment were similar to the results of the previous two reviewed studies [36, 37], which showed increased COL-1 production with a dose-dependent increase in matrix mineralization and were thus recognized as specific markers for bone resorption. Osteoblasts deposited additional woven bone (matrix) into the defect around 2 weeks after the initial implantation. Nonetheless, bone mineralization or remodeling began only once the shape of the new bone was adapted to the old tissue [38].

Bone regeneration and remodeling of treated defects were monitored by CT radiograph and histology methods. CT imaging gives three-dimensional data on bone development, whereas histology can only study a two-dimensional portion. [39].

In this investigation, macroscopic radiography evaluation revealed the existence of the biomaterial at the defect site, surrounded by a radiolucent edge in the scaffold-only group. At 3 months of healing, there was complete diminution of the radiolucent edge in the bone defects treated with hDPSCs, clearly demonstrating the shift from the reabsorption phase to the repair phase during the healing process. These findings are consistent with the earlier study [40], which found that the radiolucent edge surrounding the biomaterial-containing defects indicates an early phase of bone regeneration in which osteoclasts remove debris from the bone margins, resulting in greater regions of reabsorption. The radiolucent margins fade until they vanish completely, indicating reabsorption impairment and the start of regeneration.

Microscopically, the signals of bone regeneration were verified. After three months of a transplant, histological examination revealed that the healing symptoms of the bone deficiency in the area that received a combination of PLGA/HA scaffold and hDPSCs improved. This group was completely

regenerated and consisted of well-vascularized bone with a lamellar architecture around the Haversian canals, with a much higher cortical bone level in this area than in the scaffold-only transplant site. **Colorado et al.,** discovered that PLGA/HA scaffolds with chemical and physical characteristics improved hDPSC adhesion, growth, and differentiating towards the osteogenic lineage and encouraged critical-size osseous defect repair in vivo when used as an alternative biomaterial with hDPSc-PLGA/HA scaffold. [41]**.**

Furthermore, in the groups that only got the PLGA/HA scaffold, a more immature bone was created. The empty control group, on the other hand, showed little new bone formation with several unhealed cavities [newly formed bone marrow]. These findings are consistent with earlier research. According to **Zhang et al**., Because of its conductive action, HA has been widely used in bone scaffolds and is frequently used in clinical practise, either directly or in conjunction with other materials. Modified HA particles may aid to stabilize the mechanical properties of PLGA scaffolds by extending the calcium surface for osteoblast ossification. [42].

However, the findings of our investigation not in line with what the previous review [43] reported when HA is applied alone in a critical-size rat defect without the inclusion of stem cells, it has a higher proportion of marrow gaps and results in less bone growth than deproteinized bovine bone [DGB].

When compared to the other groups studied, immunohistochemical labeling revealed enhanced mature lamellar bone content in PLGA/HA/hDPSC-treated defects, as well as better histological feature recovery and high immunoexpression for collagen type I. This demonstrates that the higher fiber content led to good tissue quality with optimal support and structure, facilitating bone mineralization. Our results may be contrasted to those of **Pinheiro et al.,** and **Attia et al.,** who used HA/-TCP and micro-HA scaffolds, respectively. They detected an increase in collagen fiber and HA deposition, suggesting that the biomaterial caused a response in the healing process. [44, 45].

The literature now has a diverse spectrum of scaffolds targeted at helping bone undergo the critical defect repair process. Because of the parallels in functional aspects related to the

assessment of the changing kinetics of the bone repair process, the adoption of this kind of lesion has increased significantly in recent years. The HA/PLGA scaffolds have already been demonstrated, yielding intriguing results about of suitable resistance and extended residency in the lesion environment, allowing the mechanism of particle substitute by new tissue to become feasible, albeit time-consuming, as demonstrated in our work [46].

4. Conclusion

Because it was able to induce specific morphological and biological reactions that assisted in the cellular connection essential for the bone regeneration phase to occur, the innovative scaffold offered fascinating biotechnological potential. As a result, it is possible to conclude that the implantation of dental pulp stem cells resulted in a favorable reaction in the tissue environment. HDPSC cellular connectivity is necessary for bone regeneration to occur. Thus, the inclusion of dental pulp stem cells [HDPSCs] induced a favorable response in the tissue environment, and the results obtained in these groups were superior to those obtained by the scaffolds alone with HA/PLGA. However, further study is needed to confirm these benefits and to understand the molecular pathways that are activated in the early stages of the healing process.

Acknowledgments

Author Contribution

Khalaf, Afaf conceptualized the study, designed it, and wrote the primary paper. Ali, Shamaa carried out the data analysis. Sabry, Dina, Abd El Fattah, and Saher S., Mohammed helped with the drafting and revision of the text. The paper was examined by each author.

Ethical consideration

Each participant completed a permission form after being apprised of the study's procedures. As part of the ethical council's advice about the conduct of scientific research, all studies were examined and authorized in accordance with the principles for the responsible use of animals in research as a part of the scientific research ethics recommendation of the ethical Minia University **(Approval 22/2/2021: [No. 486]**

Funding

No specific grant was given to this study by funding organizations in public, private, or not-for- profit sectors.

Conflict of interest

The authors claim to have no conflicts of interest.

Availability of data & materials

Data & materials were available.

References:
1. El-Gendy, R., et al., Osteogenic differentiation of human dental pulp stromal cells on 45S5 Bioglass® based scaffolds in vitro and in vivo. Tissue Engineering Part A, 2013. 19(5-6): p. 707- 715. 2. Ito, K., et al., Osteogenic potential of effective bone engineering using dental pulp stem cells, bone marrow stem cells, and periosteal cells for osseointegration of dental implants. International Journal of Oral & Maxillofacial Implants, 2011. 26, 5
2. Ullah, I., et al., In vitro comparative analysis of human dental stem cells from a single donor and its neuronal differentiation potential evaluated by electrophysiology. Life sciences, 2016. 154: p. 39-51.
3. Jaquiéry, C., et al., In vitro osteogenic differentiation and in vivo bone-forming capacity of human isogenic jaw periosteal cells and bone marrow stromal cells. Annals of Surgery, 2005. 242(6): p. 859.
4. Liu, M. and Y. Lv, Reconstructing bone with natural bone graft: a review of in vivo studies in bone defect animal model. Nanomaterials, 2018. 8(12 :)p. 999.
5. Ranganath, S.K., et al., Bilateral double site (calvarial and mandibular) critical-size bone defect model in rabbits for evaluation of a craniofacial tissue engineering constructs. Materials Today Bio, 2022. 14: p. 100267.
6. Arthur, A., et al ,.Adult human dental pulp stem cells differentiate toward functionally active neurons under appropriate environmental cues. Stem cells, 2008. 26(7): p. 1787-1795.
7. Berbéri, A., et al., Osteogenic potential of dental and oral derived stem cells in bone tissue engineering among animal models: An update. Tissue and Cell, 2021. 71: p. 101515.
8. Collins, M.N., et al., Scaffold fabrication technologies and structure/function properties in bone tissue engineering. Advanced functional materials, 2021. 31(21 :)p. 2010609.
9. Lu, J., H. Yu, and C. Chen, Biological properties of calcium phosphate biomaterials for bone repair: A review. RSC advances, 2018. 8(4): p. 2015-2033.
10. Lansdowne, J.L., et al., Characterization of an ovine bilateral critical sized bone defect iliac wing model to examine treatment modalities based on bone tissue engineering. BioMed Research International, 2014. 2014.
11. Zwetyenga, N., et al., Mandibular reconstruction using induced membranes with autologous cancellous bone graft and HA-βTCP: animal model study and preliminary results in patients. International journal of oral and maxillofacial surgery, 2009. 38(12): p. 1289-1297.
12. Akiyama, K., et al., Lineage differentiation of mesenchymal stem cells from dental pulp, apical papilla ,and periodontal ligament. Odontogenesis: Methods and Protocols, 2012: p. 111- 121.
13. Li, J.-H., et al., Human dental pulp stem cell is a promising autologous seed cell for bone tissue engineering. 2011, Chinese Medical Journals Publishing House Co., Ltd. 42 Dongsi Xidajie …. p. 4022-4028.
14. Francia, A., et al., Establishing and implementing a simplified protocol for the expansion and culture of human dental pulp stem cells (hDPSCs). Odontoestomatología, 2021. 23(38.)
15. Zimina, A., et al., Biocompatibility and physico-chemical properties of highly porous PLA/HA scaffolds for bone reconstruction. Polymers, 2020. 12(12): p. 2938.
16. Awais, S., et al., Human dental pulp stem cells exhibit osteogenic differentiation potential. Open Life Sciences, 2020 :)1(15 .p. 229-236.
17. Kasten, P., et al., The effect of platelet-rich plasma on healing in critical-size long-bone defects. Biomaterials, 2008. 29(29): p. 3983-3992.

18. Alkaisi, A., et al., Transplantation of human dental pulp stem cells: enhance bone consolidation in mandibular distraction osteogenesis. Journal of Oral and Maxillofacial Surgery, 2013. 71(10): p. 1758. e1-1758. e13.

19. Kassir, R., A. Kolluru, and M. Kassir, Intense pulsed light for the treatment of rosacea and telangiectasias. Journal of Cosmetic and Laser Therapy, 2011. 13(5): p. 216-222.

20. Llena, C., et al., Human dental pulp stem cells exhibit different biological behaviours in response to commercial bleaching products. Materials, 2018. 11(7): p. 1098.

21. Dimitriou, R., et al ,.Bone regeneration: current concepts and future directions. BMC medicine, 2011. 9(1): p. 1-10.

22. Jazayeri, H.E., et al., A current overview of materials and strategies for potential use in maxillofacial tissue regeneration. Materials Science and Engineering: C, 2017. 70: p. 913-929.

23. Dang, M., et al., Biomimetic delivery of signals for bone tissue engineering. Bone research, 2018. 6(1): p. 25.

24. Kim, D., et al., Gingiva-derived mesenchymal stem cells: potential application in tissue engineering and regenerative medicine-a comprehensive review. Frontiers in Immunology, 2021. 12: p. 667221.

25. Park, S.H., et al., Scaffolds for bone tissue engineering fabricated from two different materials by the rapid prototyping technique: PCL versus PLGA. Journal of Materials Science: Materials in Medicine, 2012. 23: p. 2671-2678.

26. Pan, Z. and J. Ding, Poly (lactide-co-glycolide) porous scaffolds for tissue engineering and regenerative medicine. Interface focus, 2012. 2(3): p. 366-377.

27. Farahzadi, R., et al ,.Anti-aging protective effect of L-carnitine as clinical agent in regenerative medicine through increasing telomerase activity and change in the hTERT promoter CpG island methylation status of adipose tissue-derived mesenchymal stem cells. Tissue and Cell, 2018. 54: p. 105-113.

28. Fathi, E., et al., Cytokines secreted from bone marrow derived mesenchymal stem cells promote apoptosis and change cell cycle distribution of K562 cell line as clinical agent in cell transplantation. PloS one, 2019. 14(4): p .e0215678.

29. Suchánek, J., et al., Human dental pulp stem cells-isolation and long term cultivation. ACTA MEDICA-HRADEC KRALOVE-, 2007. 50(3): p. 195.

30. Kellner, M., et al., Differences of isolated dental stem cells dependent on donor age and consequences for autologous tooth replacement. Archives of Oral Biology, 2014. 59(6): p. 559- 567.

31. d'Aquino, R., et al., Dental pulp stem cells: a promising tool for bone regeneration. Stem cell reviews, 2008. 4: p. 21-26.

32. Kermani, S., et al., Differentiation capacity of mouse dental pulp stem cells into osteoblasts and osteoclasts. Cell Journal (Yakhteh), 2014. 16(1): p. 31.

33. Hilkens, P., et al., Effect of isolation methodology on stem cell properties and multilineage differentiation potential of human dental pulp stem cells. Cell and tissue research, 2013. 353(1): p. 65-78.

34. Bressan, E., et al., Donor age-related biological properties of human dental pulp stem cells change in nanostructured scaffolds. PloS one, 2012. 7(11): p. e49146.

35. Osugi, M ,.et al., Conditioned media from mesenchymal stem cells enhanced bone regeneration in rat calvarial bone defects. Tissue engineering part A, 2012. 18(13-14): p. 1479- 1489.

36. Barhanpurkar, A.P., et al., IL-3 promotes osteoblast differentiation and bone formation in human mesenchymal stem cells. Biochemical and biophysical research communications, 2012. 418(4): p. 669-675.

37. Esteves, J.C., et al., Dynamics of bone healing after osteotomy with piezosurgery or conventional drilling–histomorphometrical, immunohistochemical, and molecular analysis. Journal of translational medicine, 2013. 11(1): p. 1-13.

38. Annibali, S., et al., Histomorphometric evaluation of bone regeneration induced by biodegradable scaffolds as carriers for dental pulp stem cells in a rat model of calvarial "critical size" defect,". Journal of Stem Cell Research & Therapy, 2016. 6.

39. Nuss, K.M. and B. von Rechenberg, Biocompatibility issues with modern implants in bone-a review for clinical orthopedics. The open orthopaedics journal :2 .2118 ,p. 66.

40. Colorado, C., et al., Human recombinant cementum protein 1, dental pulp stem cells, and PLGA/hydroxyapatite scaffold as substitute biomaterial in critical size osseous defect repair in vivo. Archives of Oral Biology, 2022. 137: p. 1053.92

41. Zhang, D., et al., The development of collagen based composite scaffolds for bone regeneration. Bioactive materials, 2018. 3(1): p. 129-138.

42. Annibali, S., et al., Micro-CT and PET analysis of bone regeneration induced by biodegradable scaffolds as carriers for dental pulp stem cells in a rat model of calvarial "critical size" defect: Preliminary data. Journal of Biomedical Materials Research Part B: Applied Biomaterials, 2014. 102(4): p. 815-825.

43. Pinheiro, A.L.B., et al., Bone repair following bone grafting hydroxyapatite guided bone regeneration and infra-red laser photobiomodulation: a histological study in a rodent model. Lasers in medical science, 2009. 24: p. 234-240.

44. Attia, M.S., et al., Histological and histomorphometric evaluation of hydroxyapatite-based biomaterials in surgically created defects around implants in dogs. Journal of Periodontology, 2019. 90(3): p. 281-287.
45. Kapasa, E.R., et al., The effect of RANKL/OPG balance on reducing implant complications. Journal of functional biomaterials, 2017. 8(4): p. 42.